Aust. Met. Mag. 42 (1993) 175–182

The South Pacific and southeast Indian Ocean tropical cyclone season 1990–91

A.J. Bannister and K.J. Smith
Severe Weather Section, Western Australian Regional Office,
Bureau of Meteorology, Australia

(Manuscript received September 1993; revised September 1993)

During the 1990–91 season a total of eleven tropical cyclones affected the South Pacific and southeast Indian Ocean basins, of which five reached hurricane intensity (ten-minute mean wind speed in excess of 120 km h^{-1}). There was a total of 64 cyclone days spanning the period late November to mid-May, including 16 hurricane days. *Sina* and *Joy* caused damage costing US$55 million, accounting for over 95 per cent of the total cyclone damage in the basin. Eight lives were lost; six of these were associated with *Joy* and two with *Fifi*.

Key features of the broadscale circulation included: a more active than normal westerly monsoon in the Australian region; a weaker than normal South Pacific convergence zone (SPCZ) and an anomalously weak long wave trough over eastern Asia (with fewer cross-equatorial surges over western Indonesia and the Indian Ocean). The Madden-Julian oscillations (MJO) were weaker and less regularly defined than in the preceding two seasons. The Southern Oscillation Index (SOI) was generally negative but small. Sea-surface temperatures (SST) remained above average in the equatorial central Pacific and warm SST anomalies, although generally small, persisted in the tropical Indian Ocean.

Introduction

The Tropical Cyclone Warning Centres (TCWCs) in Brisbane, Darwin, Nadi and Perth, together with the Wellington Regional Specialised Meteorological Centre and the Climate Section, Darwin Regional Office, have provided the material to produce this report.

The 1990–91 tropical cyclone season in the South Pacific and southeast Indian Ocean basin extended from late November 1990 to the middle of May 1991. A total of eleven tropical cyclones occurred with five reaching hurricane intensity. Nine cyclones occurred in the area between 105°E and 120°W, which is seven less than the average. Eight of these were in the Australian region east of 105°E, close to the average of ten, with only one, *Sina*, in the South Pacific compared with an average of six (Rudolph and Guard 1991).

There were 64 cyclone days during the season, including 16 hurricane days. The hurricane days were spread evenly amongst five cyclones with two to four days each.

Corresponding author address: A.J. Bannister, Severe Weather Section, Bureau of Meteorology, PO Box 1370, West Perth, WA 6872, Australia.

In this summary the large-scale tropical circulation features and their effects on tropical cyclone activity during the 1990–91 season are discussed, particularly with regard to climate indices and intraseasonal oscillations. Verification statistics for the operational analyses and forecasts of tropical cyclone position are then presented together with a comparison with previous years' performances and that of the Joint Typhoon Warning Center, Guam. Finally, a brief history of each tropical cyclone is given, outlining its life cycle and the more important features.

Large-scale circulation features

Averaged over the cyclone season, the Australian westerly monsoon was more active than normal. Anomalously strong low-level westerlies were assisted by greater than normal northerly cross-equatorial flow in the region 120°E to 150°E. The upper tropospheric southeasterly return flow was also stronger than normal in this region, indicating a vigorous Hadley circulation.

To the west over Indonesia and the Indian Ocean, both the low-level equatorial northwest-

erly flow and the upper-level southeasterly return flow were weaker than normal. However the active periods that did occur were very effective in contributing to tropical cyclone development, as systems occurred in each month from December to April either in or to the west of the Australian western region.

To the east, the equatorial western Pacific had stronger than normal low-level westerly and upper-level easterly winds, associated with a stronger than normal near-equatorial trough (NET) north of the equator. The Hadley circulation was actually weaker than average in this region, and the SPCZ was weaker and located further north than is typical. Consequently there were relatively few cyclogenesis events in this region, while the northwest Pacific remained cyclone free for only the brief period between typhoon *Russ* in the last week of December and tropical storm *Sharon* in the first week of March.

Several northern hemisphere features contributed to the anomalies in the southern hemisphere westerly monsoon. The long wave trough over eastern Asia was anomalously weak with a tendency to be displaced eastwards, resulting in fewer than normal cold outbreaks and high pressure surges from China southwards into the South China Sea. Hence the northeasterly monsoon flow was weaker than average through this region, providing fewer than normal cross-equatorial surges over western Indonesia and the Indian Ocean.

In contrast to this, a region to the east of the Philippines provided a stronger than normal descending branch of the Hadley circulation. This could be identified by above average surface pressures, low-level ridging, and convergence in the upper-level flow.

Climatic indices

The SOI, defined as the normalised Tahiti minus Darwin pressure difference multiplied by ten, was generally negative but small through the cyclone season. Values fell near the end of the season to be minus 12 in April, providing an early indication of a developing El Niño event.

SSTs remained above average in the equatorial central Pacific throughout the season. This provided further evidence of a developing El Niño event. Other features consistent with a developing El Niño included persistent low-level westerly and upper divergent easterly wind anomalies over the equatorial western Pacific.

Warm SST anomalies, although generally small, persisted in the tropical Indian Ocean throughout the season. Presumably this additional forcing contributed to the steady rate of tropical cyclone formation through the season in this region. SST anomalies were generally small about the Australian tropics, and fluctuated in sign from month to month.

Intraseasonal modulation

The variations in tropical weather activity during the season were less regular and well defined than in the preceding two seasons. MJOs (Madden and Julian 1971, 1972) were prominent during the 1988–89 season (Drosdowsky and Woodcock 1991) and also during the 1989–90 season (Ready and Woodcock 1992). Two very clear MJO events occurred in the transition period leading up to the 1990–91 season. The first MJO in this period propagated eastward from the Indian Ocean to the western Pacific during late September to mid-October, the second during late October to late November.

Despite the pre-season MJO activity, no clear events occurred during the season until the period from mid-April to early May. The typical pattern of a developing MJO includes broadscale enhancement of monsoonal activity in the equatorial Indian Ocean and generally suppressed activity in the western Pacific (Rui and Wang 1990). Such a pattern was prevented by moderately active conditions in the equatorial western Pacific that persisted from mid-November through to early April.

At Australian longitudes, then, the season was not characterised by discrete monsoonal bursts separated by 40 to 50-day periods. Onset of low-level westerly winds occurred at Darwin at the average time of late December, but these were predominantly of southern hemisphere origin. It was not until January and February that the monsoon became very active and persistent across northern Australia and a vigorous Hadley circulation developed.

Although, as noted earlier, there were fewer surges in the northern hemisphere northeast monsoon than normal over the season, the number returned to near normal during January and February. Furthermore, the low frequency of vortex formation in the NET near Borneo indicated that surges which occurred in these two months penetrated across the equator more strongly than normal. This was a contributing factor to the very active Australian monsoon during January and February.

The Australian monsoon declined rapidly in March when the most active tropical weather occurred in the western Pacific, particularly north of the equator. A brief low latitude resurgence of the monsoon occurred in mid-April at which time cyclones *Marian* and *Fifi* developed. This was associated with the late season MJO that propagated eastward to the equatorial Pacific and assisted the formation of the twin systems, *Lisa* in the south and *Walt* in the north, early in May.

Verification statistics

Verification of the operational tropical cyclone analyses and forecasts is done by comparing the

Table 1. Tropical cyclone location and prediction errors compared to best track positions over the South Pacific and southeast Indian Ocean in the 1990–91 season. Error is the great circle error and number is the number of verification points. Blank indicates unavailable data.

Forecast lead time	*0 h*		*12 h*		*24 h*		*36 h*		*48 h*	
Name	*error (km)*	*number*	*error (km)*	*number*	*error (km)*	*number*	*error (km)*	*number*	*error (km)*	*number*
Chris	57	22	117	21	206	18	253	16	358	14
Daphne	24	12	81	12	225	8	344	6	509	6
Elma	26	12	147	5	234	4	335	4	271	4
Errol	76	21	152	20	189	14	271	12	361	12
Marian	54	32	137	31	229	20	324	18	432	18
Fifi	70	19	117	17	197	9	394	7	666	5
Joy	26	29	67	27	121	25	167	16	216	13
Kelvin	46	34	131	32	215	30	312	28	433	26
Lisa	26	12	96	10	177	8	286	6	438	4
Laurence	45	6	97	6						
Sina	27	27	137	23	256	20				
Total		226		204		156		113		102
Mean	43		116		205		298		409	

warning information with the 'best track' for each of the cyclones. The 'best track' is an after-the-event analysis that is performed in order to establish the most likely actual track. Often, the impact of data unavailable in operational real-time combined with the benefit of hindsight will reveal that the redrawn track or 'best track' differs from the track used operationally. The results are summarised in Table 1.

The forecasts for the 1990–91 season were more accurate than for the previous two seasons (compare a 56 km error in initial location for both the previous two seasons with a 43 km initial location error in the 1990–91 season). For the whole South Pacific and southeast Indian Ocean region the 12-hour forecast position error decreased from 139 km in the 1988–89 season to 116 km in the 1990–91 season. This was due in part to the fewer number of lower intensity cyclones where less distinct features on satellite imagery lead to poor location accuracy. With the longer lead time forecasts, large errors can occur with fast-moving cyclones, particularly when attempting to judge accurately the change in cyclone movement in response to large-scale environmental flow changes. The 24-hour forecast position error of 205 km compared favourably with the 24-hour forecast error of 211 km by the Joint Typhoon Warning Center, Guam, for the South Pacific and south Indian Ocean 1990–91 season (Rudolph and Guard 1991).

Tropical cyclones in the South Pacific and southeast Indian Oceans 1990–91

The cyclones that occurred in the South Pacific and southeast Indian Oceans during the 1990–91 season are summarised in Tables 2 and 3 and are subsequently described in greater detail in chronological order with the office that issued the warnings denoted as follows:

(B) Brisbane, Queensland, Australia
(D) Darwin, Northern Territory, Australia
(N) Nadi, Fiji
(P) Perth, Western Australia
(W) Wellington, New Zealand.

If the responsibility for a cyclone was subsequently passed to another office, then both are listed in chronological order of responsibility. The given dates represent the tropical cyclone period and all times are in UTC.

Sina (N) and (W): 24 November to 30 November 1990 (Fig. 1)

A depression that formed about 350 km northwest of Rotuma developed gale force winds by 1800, 24 November, and was codenamed *Sina*. Although moving erratically at first, *Sina* began to move slowly southwards. By late on 25 November the cyclone attained hurricane intensity, which was deduced from the appearance of an eye on satellite imagery.

At 1800, 26 November, a very distinct eye structure indicated that *Sina* had reached its maximum intensity with estimated mean winds of 140 km h^{-1}. Six hours later, when the cyclone was centred about 250 km northwest of Nadi, a progressive recurvature in its track began that took the centre close to the southwestern part of Fiji's largest island, Viti Levu. It lost hurricane intensity before passing just to the north of the island of Tongataupu in Tonga early on 29 November. For the next 24 hours or so, it moved steadily eastwards, passing about 160 km south of Niue at 0000, 30 November. Late on this same day, *Sina* ended its tropical cyclone phase as it recurved towards the southeast.

The extratropical remains of *Sina* maintained a southeastward track for two days before altering course slightly to a more southerly heading.

Table 2. Tropical cyclones of the South Pacific and southeast Indian Ocean in the 1990–91 cyclone season.

	Initial tropical low phase				*Start tropical cyclone phase*				*End tropical cyclone phase*				*Decay of tropical low*			
Name	*Date*	*Time (UTC)*	*Lat.*	*Long.*	*Date*	*Time (UTC)*	*Lat.*	*Long.*	*Date*	*Time (UTC)*	*Lat.*	*Long.*	*Date*	*Time (UTC)*	*Lat.*	*Long.*
Sina	24 Nov	1200	10.0°S	174.5°E	24 Nov	1800	10.3°S	173.8°E	30 Nov	1800	23.5°S	161.5°W	01 Dec	0000	25.4°S	159.5°W
Laurence	09 Dec	0000	11.8°S	124.9°E	10 Dec	1200	12.1°S	128.9°E	12 Dec	0000	13.3°S	127.5°E	16 Dec	0000	18.0°S	118.4°E
Joy	16 Dec	0400	11.0°S	163.0°E	19 Dec	0000	12.1°S	153.5°E	26 Dec	0600	19.5°S	147.5°E	26 Dec	2000	19.7°S	147.5°E
Chris	15 Feb	0600	15.0°S	122.0°E	16 Feb	0600	15.0°S	121.8°E	21 Feb	0000	16.7°S	111.1°E	21 Feb	1800	16.0°S	109.3°E
Daphne	20 Feb	0700	18.2°S	131.5°E	22 Feb	0600	18.9°S	121.3°E	26 Feb	0000	21.4°S	111.5°E	28 Feb	1200	28.9°S	101.5°E
Kelvin	24 Feb	0200	12.0°S	141.6°E	25 Feb	0400	15.5°S	149.0°E	05 Mar	1200	13.3°S	149.3°E	06 Mar	0000	14.2°S	150.2°E
Elma	26 Feb	0000	9.4°S	88.1°E	26 Feb	1800	11.8°S	88.6°E	03 Mar	0600	24.3°S	93.5°E	05 Mar	0000	26.0°S	89.3°E
Errol	23 Mar	1200	11.0°S	99.6°E	24 Mar	0600	11.0°S	99.5°E	29 Mar	1800	16.1°S	95.5°E	31 Mar	0600	17.4°S	92.6°E
Marian	09 Apr	0000	8.8°S	130.0°E	10 Apr	1800	10.3°S	126.0°E	17 Apr	1600	16.5°S	111.5°E	19 Apr	0000	21.3°S	108.3°E
Fifi	15 Apr	0000	10.8°S	103.2°E	16 Apr	1800	12.6°S	102.6°E	19 Apr	1800	22.5°S	105.4°E	20 Apr	0600	24.4°S	106.1°E
Lisa	07 May	0000	6.0°S	155.0°E	08 May	0000	9.0°S	155.3°E	12 May	0000	18.2°S	163.5°E	12 May	1800	20.0°S	169.8°E

Table 3. Maximum intensities of the 1990–91 season South Pacific and southeast Indian Ocean cyclones.

	Maximum estimated intensity				
Name	*Date*	*Time (UTC)*	*Lat.*	*Long.*	*Pressure (hPa)*
Sina	26 Nov	1800	15.8°S	174.4°E	960
Laurence	11 Dec	0600	13.5°S	128.2°E	996
Joy	23 Dec	0000	16.1°S	146.7°E	940
Chris	19 Feb	0000	15.8°S	116.6°E	976
Daphne	23 Feb	0600	20.1°S	115.9°E	976
Kelvin	26 Feb	1700	16.6°S	150.6°E	980
Elma	28 Feb	1800	18.0°S	88.9°E	965
Errol	26 Mar	0600	11.2°S	100.6°E	950
Marian	13 Apr	0000	13.4°S	120.2°E	930
Fifi	17 Apr	1800	14.5°S	102.2°E	975
Lisa	10 May	0600	15.5°S	156.1°E	975

Eventually it was absorbed by an advancing high latitude trough near 50°S late on 4 December. *Sina* caused no loss of human life. Fiji sustained US$18.5 million worth of damage, nearly 80 per cent of which was accounted for by losses to sugar cane, pine forests and agriculture. Tonga, Niue and the southern Cook Islands sustained minor damage.

***Laurence* (D): 10 to 12 December 1990 (Fig. 2)**

Tropical cyclone *Laurence* was the first cyclone to be named by the northern region since *Kay* (April 1987).

Large-scale mid-latitude forcing from both hemispheres occurred prior to the genesis of *Laurence*, in the form of a northeast surge in the South China Sea following a 1062 hPa Siberian high at the end of November, and strong anticyclogenesis over central Australia on 7 December.

A cloud cluster developed over the Timor Sea on 8 December. This tracked east-southeast and by the evening of 10 December it had developed into a weak tropical cyclone that was detectable at a distance of 230 km on the Darwin radar. It then moved south-southwest until 11 December when it moved west.

Fig. 1 Track of cyclone *Sina*. ○ bounds each disturbance; ● bounds the tropical cyclone phase; □ identifies maximum intensity.

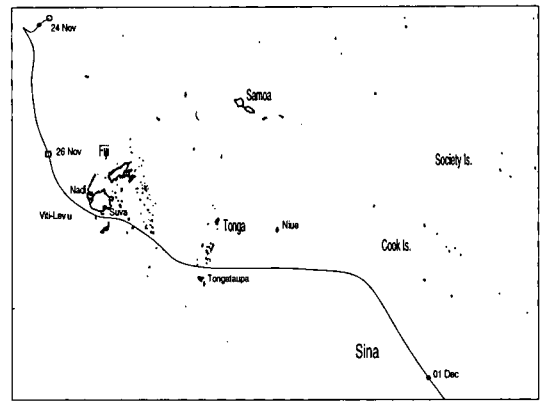

Fig. 2 Tracks of cyclones *Laurence*, *Chris*, *Daphne* and *Marian*. Symbols as in Fig. 1.

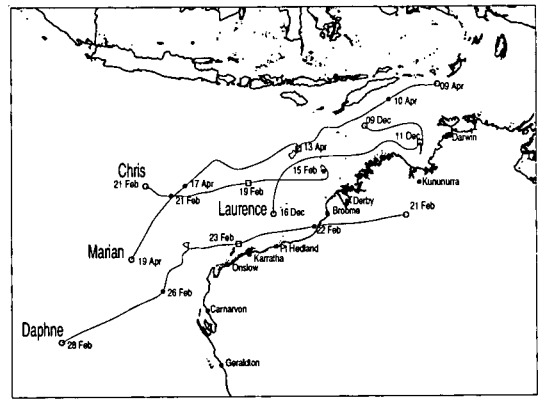

Late on 11 December, *Laurence* weakened below tropical cyclone strength under the influence of vertical wind shear from low-level easterlies. The remnants continued to track west and then south before dissipating near Rowley Shoals on 16 December.

The only report of damage was the sinking of a small fishing trawler on 11 December, however, since the trawler was 150 km away from the cyclone centre and the radius of gales was less than 55 km, the strong winds and heavy seas reported were not considered directly due to the cyclone itself.

***Joy* (B): 19 to 26 December 1990 (Fig. 3)**

A low developed east of Honiara on 15 December in response to the formation of typhoon *Russ* in the northern hemisphere. Deepening slowly over the next two days, the low headed south of the Solomon Islands and by 0000, 19 December, it was upgraded to tropical cyclone status. *Joy* proceeded on a westward path for two days before altering course to the southwest on 20 December. The cyclone underwent rapid intensification as it emerged from beneath strong upper tropospheric east to northeasterly winds and came closer to the subtropical jetstream. *Joy* reached peak intensity of 940 hPa at 0000, 23 December, with maximum sustained winds of 170 km h^{-1} when it was centred 130 km northeast of Cairns.

On 24 and 25 December, *Joy*'s movement became slow and erratic. During this period, its centre passed within 100 km of Cairns and 80 km of Green Island where a wind gust of 180 km h^{-1} was recorded. At the time of this gust, radar imagery suggested the radius of maximum winds to be 20 to 25 km. Significant structural damage occurred between Port Douglas and Innisfail on exposed parts of the coast and on offshore islands. Drier air began gradually to penetrate the central region of the cyclone and *Joy* began to lose intensity slowly.

Just after 0600, 26 December, *Joy* crossed the coast near Townsville with a central pressure of 983 hPa. At the time relatively light winds surrounded the cyclone, however, some 100 km further down the coast a band of storm force winds caused damage in the Mackay area. These winds were associated with a strong pressure gradient under the main rain-band south of the cyclone.

At about 2100, 26 December, a tornado caused extensive structural damage in a suburb of Mackay, after *Joy* crossed the coast. *Joy* and its subsequent rain depression produced widespread flooding in northern and central Queensland. Several rainfall stations in the Mackay and Pioneer Valley districts recorded more than two metres of rain between 23 December and 7 January.

Fig. 3 Tracks of cyclones *Joy*, *Kelvin* and *Lisa*. Symbols as in Fig. 1.

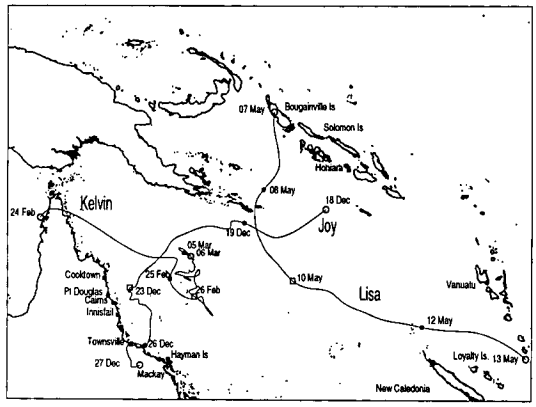

The Insurance Council of Australia advised that claims for damage attributable to *Joy* totalled $62 million. Six lives were lost; five drowned in swollen rivers and one drowned at sea.

***Chris* (P): 15 to 21 February 1991 (Fig. 2)**

During mid-February, a middle-level circulation developed over the inland Kimberley and drifted slowly westward. At 0000, 15 February, a surface low was analysed near 15.5°S 122.5°E, which subsequently deepened and was named *Chris* at 0600, 16 February, when it was near 15°S 121.8°E, 170 km off the northwest Kimberley coast. *Chris* initially moved slowly north before changing course to the southeast around 0000, 17 February. The cyclone maintained this direction for 12 hours before tracking to the west at around 1200. The centre location and intensity during this period was based on Automatic Weather Station and ship observations. Gales associated with the monsoonal northwesterly flow extended more than 370 km to the north of the cyclone.

From 0000, 18 February, the low-level centre began moving under deep convection and intensification began. An increase in forward speed of movement occurred as the system came under the increasing influence of the middle-level steering flow. Peak intensity was attained around 0000, 19 February, when the central pressure was estimated to be 976 hPa, giving probable sustained wind speeds of 110 km h^{-1}. By 1500, 19 February, *Chris* began to weaken due to strengthening easterly winds aloft. Low-level cloud features became exposed to the east of the deep convection and the speed of movement decreased.

Chris weakened below tropical cyclone strength soon after 0000, 21 February, when a well exposed centre was evident. It continued to weaken and the remaining low-level circulation centre was eventually steered northwest by a developing high pressure ridge in the middle latitudes.

***Daphne* (P): 22 to 25 February 1991 (Fig. 2)**
While cyclone *Chris* was weakening over waters to the northwest of Australia, a monsoon depression was being monitored near the Gulf of Carpentaria. The low moved towards the Queensland coast before moving westward on the northern side of the subtropical ridge axis, at a steady pace of 5° of latitude per day. It produced signficant rainfall over the Top End and Kimberley regions before reaching the coast about 100 km south of Broome. Antecedent rain in the central and eastern Kimberley combined with this event to cause the worst floods on record around Fitzroy Crossing.

Intensification of the low was rapid once it moved over water and it was named *Daphne* at 0600, 22 February. It continued its westward movement, parallel to the coast and about 100 km offshore, tracked by radar. Due to its proximity to land and a sheared upper-wind environment, the cyclone was never able to strengthen significantly, and maximum intensity was reached at 0600, 23 February, with an estimated central pressure of 976 hPa. Gales were recorded briefly at Mandora Station and Karratha but no damage was reported.

From late on 23 February several changes took place in the environment surrounding the cyclone and consequently it slowed, sheared and weakened as a developing high pressure ridge caused significant pressure rises over waters to its west. The high pressure ridge impeded the progress of *Daphne* for 36 hours, during which time the cyclone completed a clockwise loop. The ridge was then eroded by the approach of a cold frontal system, allowing *Daphne* to resume moving to the south-southwest. However, weakening was ongoing due to increasing vertical wind shear and *Daphne* was downgraded to a tropical low early on 26 February. The remnants continued to track southwest before dissipating near 30°S.

***Kelvin* (B): 25 February to 5 March 1991 (Fig. 3)**
Kelvin spent nearly all of its life describing an erratic path over the Coral Sea. It drew its origin from a depression that had formed over the Gulf of Carpentaria close to Cape York Peninsula. This low moved into the Coral Sea, intensified, and was named at 0400, 25 February, when centred near 15.5°S 149°E.

That night it passed within 80 km of Willis Island where a southerly wind gust of 156 km h^{-1} was recorded. The central pressure of the cyclone at the time was estimated to be 990 hPa. It reached its lowest estimated central pressure of 980 hPa around 1700, 26 February, and spent the next six days pursuing a very erratic course through the central Coral Sea area, before ending its tropical cyclone phase at 1200, 5 March.

For all of its life, *Kelvin* exhibited a sheared type of cloud signature with a distinct low-level cloud centre visible on satellite imagery near the eastern edge of the convective cloud.

Kelvin filled very quickly on 6 March as a new depression became established well to the southeast of Willis Island. In spite of moving close to Willis Island on two occasions, there were no reports of any significant damage.

***Elma* (P): 26 February to 3 March 1991 (Fig. 4)**
Tropical Cylcone *Elma* developed from an area of enhanced convection near 9°S 88°E on 26 February. It reached cyclone status by 1800, 26 February, and moved steadily southwards over the next few days as it intensified further.

A ship reported gales within 110 km of the cyclone centre, which was near 15.6°S 89.7°E, about 0000, 1 March. *Elma* was estimated to be at peak strength at this time with a central pressure of about 965 hPa.

The path of *Elma* then deviated to the southeast, in response to the approach of an upper trough associated with a mid-latitude frontal system of moderate intensity. During this time it started to shear apart as the upper-level northwesterly winds increased. *Elma* had weakened below cyclone strength by 0000, 3 March, before weakening further over the next couple of days as it was pushed westward by a surge in the low-level easterly flow emanating from a strengthening ridge to the south.

***Errol* (P): 24 to 29 March 1991 (Fig. 4)**
Tropical cyclone *Errol* began as a tropical low near 11°S 99.6°E at 1200, 23 March, approximately 370 km northeast of Cocos Islands. By 1200, 24 March, the low had intensified to cyclone strength.

From this time onwards development was rapid and an eye was first evident on satellite imagery at 0600, 25 March. The cyclone was estimated to be at peak strength at 0600, 26 March, with a central pressure near 950 hPa when located at 11.2°S 100.6°E. In the following 24 hours the cyclone moved towards the southeast. Strengthening upper westerlies from about 0000, 28 March, when the centre was near 13.7°S 101.8°E, caused an increase in vertical wind shear over the cyclone. The low-level centre became increasingly exposed and moved towards the west whilst weakening.

Errol formed in a col area between upper-level anticyclones and was slow moving during the period of its intensification from 23 to 26 March. It then moved south of the upper ridge axis in the southwest quadrant of the dominant upper-level anticyclone. In so doing it moved into a region of stronger westerly winds (55–75 km h^{-1}) and was sheared apart. The shallow remnant circulation was then steered westward by easterly winds associated with a low-level anticyclone to the south.

Fig. 4 Tracks of cyclones *Elma*, *Errol* and *Fifi*. Symbols as in Fig. 1.

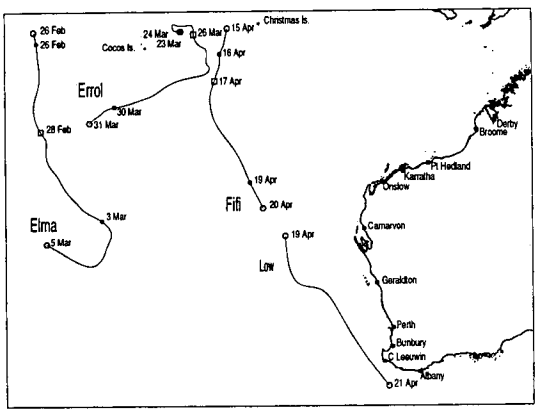

***Marian* (P): 10 to 16 April 1991 (Fig. 2)**

Severe tropical cyclone *Marian* was first evident as a middle-level depression over the western Arafura Sea. In response to a southeasterly surge and a weaker monsoonal surge, it intensified to cyclone strength about 110 km south of Timor, under a divergent upper northeasterly wind regime.

Its initial development may have been inhibited by restrictions to its low-level inflow caused by the mountains of Timor to its north. Once clear of this barrier, the cyclone intensified rapidly as it continued to move west-southwest, under the influence of a subtropical high over Australia. It moved slowly and erratically between 13 and 16 April as a new middle-level ridge developed to its west. Its peak estimated intensity of 930 hPa was reached during this period and weakening commenced as vertical shear increased across the system.

For a period of about one day, commencing 1000, 13 April, Tropical Cyclone Watch advices were issued for parts of the Pilbara and Kimberley coastline. These advices were cancelled when the shearing process become apparent.

Marian weakened further as its remnants drifted southwest before being absorbed into the circulation associated with cyclone *Fifi*.

***Fifi* (P): 16 to 19 April 1991 (Fig. 4)**

Tropical cyclone *Fifi* formed from an active area in the monsoon trough near 11°S 103°E, assisted by a southeasterly surge associated with the passage of a major subtropical high to the south.

The incipient low moved only slowly at first and attained cyclone strength at about 1800, 16 April. It then moved steadily southwards through a break in the middle-level ridge and intensified.

Fifi was estimated to be at peak intensity of about 975 hPa between 1800, 17 April, and 0600, 18 April. During 19 April, a trough line incorporating the remnants of *Marian* was evident extending southeastwards from the cyclone centre. As this trough developed, *Fifi* began to shear due to strengthening upper-level northwesterly winds ahead of a large-amplitude slow-moving cold front which approached from the west. Gales associated with *Fifi* were estimated to have ceased around 1800, 19 April, when the centre was near 22.5°S 105.4°E.

At 2100, 19 April, another cyclonic circulation became visible on satellite imagery near 25.7°S 107.7°E, approximately 370 km to the southeast of the rapidly weakening *Fifi*. The new low appears to have been the result of a baroclinic process that developed in response to the increasing thermal and moisture gradients between *Fifi* and the cold front to the west. This low moved south-southeast during 20 April, then accelerated and intensified during 21 April, passing within 100 km of Cape Leeuwin at 0700.

Gale force winds occurred over coastal waters from Jurien Bay to Bremer Bay and a brief period of storm force winds occurred as the low passed the southwest capes. Mean winds over land were near gale force for a period of about four hours, producing a period of extreme fire weather conditions. A pall of thick dust blanketed most of the southwest region, reducing visibility to 200 m at times. A total of 27 fires were reported over the southwest.

Two deaths were attributed to the gale force winds and damage in the Perth area exceeded $1 million.

***Lisa* (B), (N) and (W) 8 to 12 May 1991 (Fig. 3)**

A tropical low developed near Bougainville Island on 7 May. By 0000, 8 May, satellite imagery indicated that this depression had formed into a tropical cyclone. *Lisa* continued to intensify as it moved across the axis of an upper tropospheric ridge and closer to a strong upper subtropical west-northwesterly jet stream. The cyclone began recurving towards the southeast soon after entering the Coral Sea, reaching peak intensity near 15.5°S 156.1°E at 0600, 10 May, with a central pressure estimated at 975 hPa and sustained winds of 110 km h^{-1}. From satellite imagery it maintained this intensity for a little over 24 hours after which time it weakened rapidly as it moved closer to the subtropical jet. By the time *Lisa* passed over Anatom at about 1800, 12 May, it had ended its tropical low phase.

Once former tropical cyclone *Lisa* had crossed 25°S, it recurved slightly to the east. On 14 May, this transformed low began to deepen under the influence of an upper-level mid-latitude trough. This regenerative process was explosive between 0000 and 0600, 15 May, when the central pressure was estimated to have fallen about 10 hPa. The system tracked southeastwards and weakened slowly. It became slow moving on 20 and 21 May before dissipating near 50°S 130°W

Acknowledgments

The authors wish to acknowledge the staff of the Australian Bureau of Meteorology's TCWCs as well as those of the Fiji and New Zealand Meteorological Services. The descriptions of each cyclone were submitted by the staff of the offices responsible for issuing of warnings.

The climatological summaries were prepared by Russell Stringer of the Climate Section, Darwin Regional Office. Gary Foley and Barry Hanstrum provided many useful comments.

References

Drosdowsky, L. and Woodcock, F. 1991. The South Pacific and southeast Indian Ocean tropical cyclone season 1988–1989. *Aust. Met. Mag., 39*, 113–29.

Dvorak, V.F. 1984. Tropical cyclone intensity analysis using satellite data. *NOAA Tech. Rep. NESDIS 11*, 47 pp.

Madden, R.A. and Julian, P.R. 1971. Detection of a 40–50 day oscillation in the zonal wind in the tropical Pacific. *J. Atmos. Sci., 28*, 702–7.

Madden, R.A. and Julian, P.R. 1972. Description of global-scale circulation cells in the tropics with a 40–50 day period. *J. Atmos. Sci., 29*, 1109–23.

Ready, S. and Woodcock, F. 1992. The South Pacific and southeast Indian Ocean tropical cyclone season 1989–1990. *Aust. Met. Mag., 40*, 111–21.

Rudolph, D.K. and Guard, C.P. 1991. *Annual Tropical Cyclone Report*. U.S. Naval Oceanography Command Center/Joint Typhoon Warning Center, COMNAVMARIANAS, Box 12 FPO, AP 96540-0051, USA.

Rui, H. and Wang, B. 1990. Development characteristics and dynamic structure of tropical intraseasonal convection anomalies. *J. Atmos. Sci., 47*, 357–79.

Appendix

Sources of data:

Darwin Tropical Diagnostic Statement, November 1990 to May 1991. Available from the Northern Territory Regional Office, Bureau of Meteorology, PO Box 735, Darwin 0801, Australia.

Monthly Report on Climate System, November 1990 to April 1991. Available from the Long-range Forecast Division, Forecast Department, Japan Meteorological Agency, 1–3–4 Otemachi Chiyoda-ku, Tokyo 100, Japan.

Climate Diagnostics Bulletin, November 1990 to April 1991. Available from the Climate Analysis Center, W/NMC52, World Weather Building, Room 605, 5200 Auth Road, Washington, D.C. 20233.